to about 100 cm^{-1}, diagnostic of bidentate coordination by the carboxylate groups.[4] When the 6-coordinate complexes are dissolved in alcohol, this separation goes up to about 190 cm^{-1}, indicative of monodentate coordination by the carboxylate moieties in solution.

The 6-coordinate structures are best described as having highly distorted octahedral coordination polyhedra. The principal distortion occurs because of the small bite size of the bidentate carboxylate ligands, the two Co–O bonds of which subtend angles of about 60° at the cobalt atom. The structure of $[Co(OAc)_2(2\text{-}Me\text{-}Im)_2]$ (Figure 1) might best be described as having an equatorial plane consisting of O1A, N1B, O1B, and O2A with axial ligation by O2B and N1B. Note that the O2B–Co–N1A angle (161.6°) deviates considerably from the 180° angle of idealized octahedral geometry. The coordination polyhedron for $[Co(bu)_2(2\text{-}Me\text{-}Im)_2]$ is quite similar (Figure 3), although the structures are not isomorpohous and in this case the cobalt atom lies on a special position of C_2 symmetry. A description of the 6-coordinate structures in terms of a pseudotetrahedral model is unsatisfactory. The positions of the two liganding imidazole nitrogen atoms and the centers of the bites of the two carboxylate ligands form an extremely poor tetrahedron.

The expected increase in the effective ionic radius upon increasing the coordination number from 4 to 6 is observed. The effect is slight for the Co–N bonds, which increase an average of only 0.03 Å on going to the higher coordination number. The effect is much more pronounced, however, for the carboxylate coordination in which the two carboxylate oxygen atoms are not bonded equally. In the 6-coordinate structures the shorter of the C–O bonds average 2.11 Å while the longer set average 2.28 Å. These distances are to be compared with an average value of 1.97 Å for the Co–O bonds in the 4-coordinate structures, which involved monodentate coordination. In the 4-coordinate structures the nonbonded Co–O distances range from 2.63 to 3.05 Å. It is perhaps significant that in the 6-coordinate structures the longer of the two Co–O bonds is in each case trans to an imidazole ligand, while the shorter Co–O bond is trans to another Co–O bond.

In summary, the present structural studies have uncovered a novel type of linkage isomerism. Our results suggest that the free energy difference between 4- and 6-coordinate structures of this type is extremely small and that the actual structure adopted will depend upon crystal-packing forces. In solution it appears that 4-coordination is favored. Further evidence is presented regarding the great similarity and general lack of stereochemical preference for 4-coordinate complexes of both cobalt(II) and zinc(II), which are intended to mimic the active-site geometry of certain metalloenzymes.

Acknowledgment. This research was supported by the National Science Foundation through Grant CHE-7919581.

Registry No. $Co(C_2H_3O_2)_2(CH_3C_3N_2H_3)_2$, 74194-12-0; $Co(C_3H_5O_2)_2(CH_3C_3N_2H_3)_2$, 82281-51-4; $Co(C_4H_7O_2)_2(CH_3C_3N_2H_3)_2$, 82281-52-5; $Co(C_2H_3O_2)_2(C_2H_5C_3N_2H_3)_2$, 82265-73-4.

Supplementary Material Available: Listings of H atom positional parameters, bond distances and angles, thermal parameters (Tables A–K), positional and thermal parameters, and structure factor amplitudes (63 pages). Ordering information is given on any current masthead page.

---

[4] Robinson, S. D.; Uttley, M. F. *J. Chem. Soc.* **1973**, 1912.

Contribution from the Departments of Chemistry, West Virginia University, Morgantown, West Virginia 26506,
and Wichita State University, Wichita, Kansas 67208

Comparison of the Molecular Structures of Five-Coordinate Copper(II) and Zinc(II) Complexes of 2,6-Diacetylpyridine Dioxime[1]

GARY A. NICHOLSON,[2a] JEFFREY L. PETERSEN,*[2a] and B. JACK McCORMICK*[2b]

Received December 22, 1981

X-ray diffraction studies of $Cu(DAPDH_2)Cl_2{\cdot}2H_2O$ and $Zn(DAPDH_2)Cl_2{\cdot}H_2O$, where $DAPDH_2$ is 2,6-diacetylpyridine dioxime, were performed to determine the molecular configurations of these five-coordinate complexes. In both compounds $DAPDH_2$ behaves as a tridentate ligand. For $Cu(DAPDH_2)Cl_2$ the metal coordination geometry resembles a distorted square pyramid with C_s-m symmetry, whereas for $Zn(DAPDH_2)Cl_2$ it can be viewed roughly as a distorted trigonal bipyramid with C_{2v}-$mm2$ symmetry. The susceptibility of $Cu(DAPDH_2)Cl_2$ to second-order Jahn–Teller distortions is reflected by the ca. 0.24-Å difference in the apical and basal Cu–Cl bonds of 2.463 (1) and 2.220 (1) Å, respectively. A comparison of the M–N(oxime) and M–N(py) bond lengths reveals that these bonds are ca. 0.13 and 0.20 Å longer in $Zn(DAPDH_2)Cl_2$ than the respective bonds in $Cu(DAPDH_2)Cl_2$. In contrast, the basal Cu–Cl bond distance in $Cu(DAPDH_2)Cl_2$ is comparable in magnitude to the Zn–Cl distances in $Zn(DAPDH_2)Cl_2$. These results suggest that the directional orientation of the available metal orbitals with respect to the dioxime's N donor orbitals leads to poorer angular overlap in the five-coordinate Zn complex. $Cu(DAPDH_2)Cl_2{\cdot}2H_2O$ crystallizes in the centrosymmetric triclinic space group $P\bar{1}$ with refined lattice parameters of $a = 7.992$ (2) Å, $b = 10.282$ (3) Å, $c = 10.462$ (3) Å, $\alpha = 105.15$ (2)°, $\beta = 107.05$ (2)°, $\gamma = 106.43$ (2)°, $V = 730.7$ (4) $Å^3$, and $Z = 2$, whereas $Zn(DAPDH_2)Cl_2{\cdot}H_2O$ crystallizes in the centrosymmetric monoclinic space group $P2_1/n$ with $a = 10.104$ (3) Å, $b = 14.505$ (4) Å, $c = 9.768$ (2) Å, $\beta = 103.90$ (2)°, $V = 1394.5$ (6) $Å^3$, and $Z = 4$. Full-matrix least-squares refinement (based on F_o^2) of diffractometry data with $F_o^2 > \sigma(F_o^2)$ converged to final discrepancy indices of $R(F_o) = 0.026$, $R(F_o^2) = 0.038$, and $\sigma_1 = 1.53$ for $Cu(DAPDH_2)Cl_2{\cdot}2H_2O$ and $R(F_o) = 0.035$, $R(F_o^2) = 0.049$, and $\sigma_1 = 1.61$ for $Zn(DAPDH_2)Cl_2{\cdot}H_2O$.

Introduction

Structural studies have been performed on a wide variety of transition-metal oxime complexes to examine the possible metal-coordination modes associated with oxime ligands and their subsequent influence upon the geometry of the metal complex.[3] In particular, a systematic investigation of the coordination chemistry of 2,6-diacetylpyridine dioxime, $DAPDH_2$, with Cu(II) has led to the isolation and characterization of a monomeric species, $Cu(DAPDH_2)Cl_2$, and the tetrafluoroborate salt of the binuclear copper cation, [Cu-

---

[1] This paper is based in part upon a dissertation submitted by G. A. Nicholson to the Graduate School of West Virginia University in partial fulfillment of the requirements for the Ph.D. degree, Nov 1980.

[2] (a) West Virginia University. (b) Wichita State University.

[3] Chakravorty, A. *Coord. Chem. Rev.* **1974**, *13*, 1.

0020-1669/82/1321-3274$01.25/0 © 1982 American Chemical Society

$(DAPDH)]_2^{2+}$.[4] An X-ray diffraction analysis of the latter complex[5] revealed that the coordination environment about each Cu(II) center consists of three oxime N donors from one oxime ligand and a deprotonated oxime O donor from the other oxime ligand. These donor atoms are located at the basal corners of a square pyramid with the apex occupied by a water of hydration. The two Cu centers, which are separated by 3.5453 (7) Å, are weakly coupled with a bulk magnetic moment of 0.6 μ_B per metal. Whereas the deprotonated oxime ligand, $DAPDH^-$, interacts as a tetradentate ligand in this binuclear cation, solution conductivity measurements[4,6] suggest that the fully protonated form, $DAPDH_2$, behaves as a tridentate ligand in both of the neutral monomers, $Cu(DAPDH_2)Cl_2$ and $Zn(DAPDH_2)Cl_2$. Consequently, we have undertaken X-ray diffraction analyses of $Cu(DAPDH_2)Cl_2 \cdot 2H_2O$ and $Zn(DAPDH_2)Cl_2 \cdot H_2O$ to establish the coordination geometry about the metal and to examine the structural parameters associated with the oxime's mode of coordination in each case. In addition, since Cu(II) complexes are quite susceptible to Jahn–Teller distortions whereas Zn(II) complexes are not, these structural determinations have provided an opportunity to determine the degree to which the coordination geometry in these unusual five-coordinate complexes is affected by the electronic configuration of the metal ion. Therefore, this study not only contributes to our fundamental understanding of the stereochemistry of Cu(II) and Zn(II) oxime complexes but also adds to the limited structural data base available for low-symmetry copper and five-coordinate zinc complexes.

Experimental Section

Materials and Analyses. The chemicals were of reagent grade and were used without further purification. C, H, and N analyses were performed by Galbraith Microanalytical Laboratories. Aldrich Chemical Co. supplied the 2,6-diacetylpyridine.

Instrumentation. Infrared spectra of the complexes mulled with Nujol were measured with a Beckman IR-12 spectrometer. Conductivity measurements and titrations were made with the same procedures and equipment as described earlier.[4]

Preparation of $Cu(DAPDH_2)Cl_2$. $Cu(DAPDH_2)Cl_2$ was prepared by a previously described method.[4] Suitable crystals of the dihydrate for the X-ray diffraction analysis were obtained by the cooling of a saturated methanol solution.

Preparation of $Zn(DAPDH_2)Cl_2$. To a solution of 0.198 g (1.45 mmol) of $ZnCl_2$ in 15 mL of ether was added 0.28 g (1.45 mmol) in $DAPDH_2$. The white solid was collected, washed with three 10-mL portions of ether, and dried in vacuo. Anal. Calcd for $Zn(C_9H_{11}N_3O_2)Cl_2$: C, 32.81; H, 3.37; N, 12.75. Found: C, 32.75; H, 3.50; N, 12.64. The compound is soluble in water and polar organic solvents but is insoluble in nonpolar organic solvents. The molar conductance of a 1×10^{-3} M nitromethane solution yields a value for Λ_m of 4.8 Ω^{-1} cm^2 mol^{-1}, which is consistent with a five-coordinate complex. The infrared spectrum shows ν_{OH} centered at 3420 cm^{-1}, ν_{CN} at 1605 cm^{-1}, and ν_{NO} at 1090 cm^{-1}. Aqueous solutions of $Zn(DAPDH_2)Cl_2$ are acidic, and the titration curve exhibits one inflection corresponding to the deprotonation of an acidic proton of the coordinated oxime ligand and subsequent formation of a finely divided white precipitate.

Attempts to recrystallize $Zn(DAPDH_2)Cl_2$ from methanol, however, led to crystals which slowly lose solvent upon standing. However, controlled evaporation of solvent in air from a saturated nitromethane/THF solution eventually proved to be a satisfactory method for crystallization of the monohydrated complex.

Data Collection. The same general procedure was employed to collect the X-ray diffraction data for $Cu(DAPDH_2)Cl_2 \cdot 2H_2O$ and $Zn(DAPDH_2)Cl_2 \cdot H_2O$. Each crystalline sample was wedged inside a thin-walled capillary tube with the crystal growth axis nearly parallel to the spindle axis of the goniometer. The samples were transferred to a Picker goniostat which is operated by the computer control of a Krisel Control diffractometer automation system. A preliminary search for low-angle reflections ($2\theta = 5{-}10°$) provided a sufficient number of reflections in each case to use an autoindexing routine[7] to determine the lattice parameters of the reduced unit cell. From the unrefined orientation matrix, ω, χ, and 2θ for 20 higher order reflections were calculated, optimized by the automatic peak-centering algorithm,[8] and least-squares fit to provide the corresponding refined lattice parameters in Table I and the orientation matrix.

Table I. Data for the X-ray Diffraction Analyses of $Cu(C_9H_{11}N_3O_2)Cl_2 \cdot 2H_2O$ and $Zn(C_9H_{11}N_3O_2)Cl_2 \cdot H_2O$

	$Cu(C_9H_{11}N_3O_2)Cl_2 \cdot 2H_2O$	$Zn(C_9H_{11}N_3O_2)Cl_2 \cdot H_2O$
	(A) Crystal Data	
cryst syst	triclinic	monoclinic
space group	$P\bar{1}$ (C_i^1, No. 2)	$P2_1/n$ (nonstandard setting of $P2_1/c$ (C_{2h}^5, No. 14))
a, Å	7.992 (2)	10.140 (3)
b, Å	10.282 (3)	14.505 (4)
c, Å	10.462 (3)	9.768 (2)
α, deg	105.15 (2)	90
β, deg	107.05 (2)	103.90 (2)
γ, deg	106.43 (2)	90
V, Å^3	730.7 (4)	1394.5 (6)
fw	363.98	347.50
d(obsd), g/cm^3	1.66	1.66
d(calcd), g/cm^3	1.65	1.655
Z, formula units/unit cell	2	4
μ, cm^{-1}	19.3	22.4
	(B) Data Collection and Analysis Summary	
cryst dimens, mm	$0.25 \times 0.125 \times 0.10$	$0.35 \times 0.175 \times 0.35$
reflctns sampled	$h,\pm k,\pm l$ ($5° < 2\theta < 45°$)	$\pm h,k,l$ ($3° < 2\theta < 50°$)
2θ range for centered reflctns, deg	27–34	30–38
scan-width parameters	$A = 1.2; B = 0.7$	$A = 1.0; B = 0.9$
no. of std reflctns	3	3
% cryst decay	7	2
total no. of measd reflctns	2152	2623
no. of unique data used	1803 ($F_o^2 > \sigma(F_o^2)$)	2206 ($F_o^2 > \sigma(F_o^2)$)
agreement between equiv data		
$R_{av}(F_o)$	0.012	0.012
$R_{av}(F_o^2)$	0.018	0.009
transmission coeff	0.77–0.83	0.50–0.67
P	0.035	0.030
$R(F_o)$	0.026	0.035
$R(F_o^2)$	0.038	0.049
$R_w(F_o^2)$	0.069	0.074
σ_1, error in observn of unit wt	1.53	1.61
no. of variables	225	215

Intensity data were measured with Zr-filtered Mo Kα X-ray radiation ($\lambda(K\alpha_1) = 0.709\,26$ Å, $\lambda(K\alpha_2) = 0.713\,54$ Å) at a take-off angle of 2°. Each diffraction peak was scanned at a fixed rate of 2°/min with use of the $\theta{-}2\theta$ scan mode and variable scan widths calculated from the expression $w = A + B \tan \theta$. Background counts of 10-s duration were measured at the extremes of each scan with the crystal and counter kept stationary. The pulse-height analyzer of the scintillation detector was adjusted to accept 90% of the diffracted peak. During data collection the intensities of three standard reflections were measured periodically. The integrated intensity, *I*, and its

---

(4) Nicholson, G. A.; Lazarus, C. R.; McCormick, B. J. *Inorg. Chem.* **1980**, *19*, 192.

(5) Nicholson, G. A.; Petersen, J. L.; McCormick, B. J. *Inorg. Chem.* **1980**, *19*, 195.

(6) Nicholson, G. A. Ph.D. Dissertation, West Virginia University, Morgantown, WV, 1980.

(7) The automatic reflection-indexing algorithm is based upon Jacobson's procedure: Jacobson, R. A. *J. Appl. Crystallogr.* **1976**, *9*, 115.

(8) The automatic peak-centering algorithm is similar to that described by Busing: Busing, W. R. "Crystallographic Computing"; Ahmed, F. R., Ed.; Munksgaard: Copenhagen, 1970; p 319. The ω, χ, and 2θ angles are optimized with respect to the $K\alpha_1$ peak ($\lambda = 0.709\,26$ Å).

Table II. Positional Parameters for $Cu(C_9H_{11}N_3O_2)Cl_2 \cdot 2H_2O^a$

atom	*x*	*y*	*z*
Cu	0.27199 (5)	0.30457 (4)	0.39704 (3)
Cl1	0.00909 (10)	0.06322 (8)	0.25653 (8)
Cl2	0.12360 (12)	0.45455 (9)	0.37016 (10)
O1	0.1729 (4)	0.3863 (3)	0.6601 (3)
O2	0.3555 (4)	0.3286 (3)	0.1280 (3)
WO1	0.1787 (5)	0.9059 (5)	0.0519 (4)
WO2	0.0517 (5)	0.3867 (4)	0.0380 (4)
N1	0.2817 (4)	0.3307 (3)	0.5992 (3)
N2	0.4703 (3)	0.2398 (2)	0.4740 (2)
N3	0.3958 (3)	0.2953 (3)	0.2493 (2)
C1	0.4073 (10)	0.2901 (7)	0.8219 (5)
C2	0.3906 (4)	0.2857 (3)	0.6757 (3)
C3	0.5069 (4)	0.2327 (3)	0.6048 (3)
C4	0.6446 (5)	0.1848 (4)	0.6611 (4)
C5	0.7444 (5)	0.1464 (4)	0.5804 (4)
C6	0.7100 (4)	0.1583 (3)	0.4477 (4)
C7	0.5698 (4)	0.2072 (3)	0.3969 (3)
C8	0.5209 (4)	0.2392 (3)	0.2643 (3)
C9	0.6103 (7)	0.2077 (6)	0.1608 (5)
H1	0.118 (7)	0.412 (5)	0.600 (5)
H2	0.332 (7)	0.289 (6)	0.832 (6)
H3	0.527 (6)	0.332 (5)	0.884 (5)
H4	0.374 (7)	0.193 (6)	0.814 (6)
H5	0.668 (4)	0.185 (3)	0.754 (3)
H6	0.833 (5)	0.118 (4)	0.610 (4)
H7	0.781 (4)	0.133 (3)	0.391 (3)
H8	0.660 (7)	0.143 (5)	0.165 (5)
H9	0.529 (7)	0.170 (5)	0.070 (6)
H10	0.686 (7)	0.290 (6)	0.157 (5)
H11	0.268 (5)	0.341 (3)	0.122 (4)
WH1	0.082 (7)	0.851 (6)	0.011 (6)
WH2	0.142 (8)	0.965 (6)	0.117 (6)
WH3	0.029	0.698	0.009
WH4	0.097	0.398	0.973

[a] The estimated standard deviations in parentheses for this and all subsequent tables refer to the least significant figures.

standard deviation, $\sigma_c(I)$, for each of the measured peaks were calculated from the expressions $I = w(S/t_s - B/t_b)$ and $\sigma_c(I) = w(S/t_s^2 + B/t_b^2)^{1/2}$, where S represents the total scan count measured in time t_s and B is the combined background count in time t_b. The intensity data were corrected for crystal decay, absorption, and Lorentz-polarization effects. The standard deviation of the square of each structure factor, $F_o^2 = AI/Lp$, was calculated from $\sigma(F_o^2) = [\sigma_c(F_o^2)^2 + (pF_o^2)^2]^{1/2}$. Duplicate reflections were averaged.[9] Specific details of the data collection procedure for each complex are summarized in Table I.

Table III. Positional Parameters for $Zn(C_9H_{11}N_3O_2)Cl_2 \cdot H_2O$

atom	*x*	*y*	*z*
Zn	0.07815 (3)	0.13761 (2)	0.19959 (3)
Cl1	0.24396 (8)	0.15565 (6)	0.08717 (8)
Cl2	−0.12823 (8)	0.08705 (6)	0.08587 (8)
O1	0.1744 (3)	−0.0773 (2)	0.2363 (3)
O2	−0.0169 (3)	0.3514 (2)	0.1276 (3)
N1	0.1507 (2)	0.0028 (2)	0.3017 (3)
N2	0.1100 (2)	0.1569 (2)	0.4143 (2)
N3	0.0258 (2)	0.2842 (2)	0.2282 (2)
C1	0.2287 (5)	−0.0849 (4)	0.5213 (5)
C2	0.1765 (3)	−0.0012 (2)	0.4360 (3)
C3	0.1504 (3)	0.0865 (2)	0.5031 (3)
C4	0.1650 (3)	0.0970 (3)	0.6463 (3)
C5	0.1409 (4)	0.1821 (3)	0.6970 (3)
C6	0.1014 (4)	0.2539 (3)	0.6059 (3)
C7	0.0861 (3)	0.2401 (2)	0.4632 (3)
C8	0.0413 (3)	0.3119 (2)	0.3552 (3)
C9	0.0167 (4)	0.4083 (3)	0.3953 (5)
WO	0.4347 (4)	0.2260 (3)	0.3766 (4)
H1	0.142 (4)	−0.071 (3)	0.136 (4)
H2	0.226 (6)	−0.132 (4)	0.474 (6)
H3	0.191 (4)	−0.093 (3)	0.606 (5)
H4	0.315 (5)	−0.067 (3)	0.571 (5)
H5	0.190 (4)	0.047 (3)	0.705 (4)
H6	0.152 (3)	0.188 (2)	0.798 (4)
H7	0.086 (3)	0.307 (2)	0.642 (3)
H8	0.084 (5)	0.435 (3)	0.465 (5)
H9	0.001 (4)	0.448 (3)	0.316 (4)
H10	−0.066 (5)	0.414 (3)	0.416 (5)
H11	−0.026 (4)	0.329 (3)	0.045 (4)
WH1	−0.098 (4)	0.293 (3)	−0.185 (4)
WH2	−0.095 (8)	0.220 (5)	−0.127 (7)

Structural Analyses. Approximate positions for most of the nonhydrogen atoms in $Cu(DAPDH_2)Cl_2 \cdot 2H_2O$ were interpolated from the first E map calculated with use of MULTAN 78[10] and the phase assignments for the set with the highest figure of merit. The remaining hydrogen atoms were located with difference Fourier methods. The hydrogen atoms of the second water molecule were poorly resolved and consequently included as fixed contributions to the analysis. Near the end of the structural refinement, an examination of the agreement between F_o^2 and F_c^2 for the strong reflections indicated a small systematic variation due to extinction. To correct for this effect, we introduced an isotropic secondary extinction parameter, g.[11-13] Full-matrix refinement of the positional and anisotropic thermal parameters for the 19 nonhydrogen atoms with approximate contributions for the 15 hydrogen atoms[14-19] led to the final discrepancy indices of $R(F_o) = 0.026$, $R(F_o^2) = 0.038$, and $R_w(F_o^2) = 0.069$ with $\sigma_1 = 1.53$ and $g = (1.5\ (4)) \times 10^{-5}$. The refinement was considered to be converged after the shift to error ratio for the 225 varied parameters was less than 0.10.

The crystal structure of $Zn(DAPDH_2)Cl_2 \cdot H_2O$ was determined by heavy-atom methods. The initial coordinates of the Zn atom were interpreted from the strongest peaks of an unsharpened three-dimensional Patterson map and used in subsequent Fourier summations to locate the remaining nonhydrogen atoms. A difference Fourier map calculated with low-angle data ($(\sin\theta)/\lambda < 0.40$ Å^{-1}) was used to determine the coordinates of the hydrogen atoms. Full-matrix least-squares refinement[15-19] with anisotropic temperature factors for the 18 nonhydrogen atoms and isotropic temperature factors for the 13 hydrogen atoms led to the final convergence with $R(F_o) = 0.035$, $R(F_o^2) = 0.049$, $R_w(F_o^2) = 0.074$, and $\sigma_1 = 1.61$. A final Fourier difference map in each case verified the correctness of the structural analysis.

The positional parameters obtained from the last least-squares refinement cycle are provided in Tables II and III for $Cu(DAPDH_2)Cl_2 \cdot 2H_2O$ and $Zn(DAPDH_2)Cl_2 \cdot H_2O$, respectively. The corresponding interatomic distances and bond angles and their esd's, which were calculated from the estimated standard errors of the fractional atomic coordinates, are compared in Table IV for the nonhydrogen atoms. Tables of the refined thermal parameters, the hydrogen bond distances, the specific least-squares planes, and the observed and calculated structure factors for $Cu(DAPDH_2)Cl_2 \cdot 2H_2O$ and $Zn(DAPDH_2)Cl_2 \cdot H_2O$ are available as supplementary material.[20]

---

(9) $R_a(F_o) = \sum|F_o(\mathrm{av}) - |F_o||/\sum F_o$ and $R_a(F_o^2) = \sum|F_o^2(\mathrm{av}) - F_o^2|/\sum F_o^2$.

(10) DeClerq, J. P.; Germain, D.; Main, P.; Woolfson, M. M. *Acta Crystallogr., Sect. A* **1973**, *A29*, 231.

(11) The Zachariasen approximation[12] was employed for the overall isotropic extinction parameter, g, as defined and scaled by Coppens and Hamilton.[13]

(12) Zachariasen, W. H. *Acta Crystallogr., Sect. A* **1967**, *A23*, 558.

(13) Coppens, P.; Hamilton, W. C. *Acta Crystallogr., Sect. A* **1970**, *A26*, 71.

(14) The positional and isotropic temperature parameters for all of the hydrogen atoms, except the two water hydrogens associated with O4, were varied during the least-squares refinement. The poorer resolution of the hydrogen atoms observed for this second water molecule reflects the presence of either a disorder or an excessive thermal motion.

(15) The least-squares refinement[16] of the X-ray diffraction data was based upon the minimization of $\sum w_i|F_o^2 - S^2F_c^2|$, where w_i is the individual weighting factor and S is the scale factor. The discrepancy indices were calculated from the expressions $R(F_o) = \sum||F_o| - |F_c||/\sum|F_o|$, $R(F_o^2) = \sum|F_o^2 - F_c^2|/\sum F_o^2$, and $R_w(F_o^2) = [\sum w_i|F_o^2 - F_c^2|^2/\sum w_i F_o^4]^{1/2}$ where n is the number of parameters varied during the last refinement cycle.

(16) The scattering factors utilized in all calculations were those of Cromer and Mann[17] for the nonhydrogen atoms and those of Stewart et al.[18] for the hydrogen atoms with corrections included for anomalous dispersion.[19]

(17) Cromer, D. T.; Mann, J. *Acta Crystallogr., Sect. A* **1968**, *A24*, 231.

(18) Stewart, R. F.; Davidson, E. R.; Simpson, W. T. *J. Chem. Phys.* **1965**, *42*, 3175.

(19) Cromer, D. T.; Liberman, D. *J. Chem. Phys.* **1970**, *53*, 1891.

(20) The computer programs that were used for the structural analysis are described elsewhere.[5]

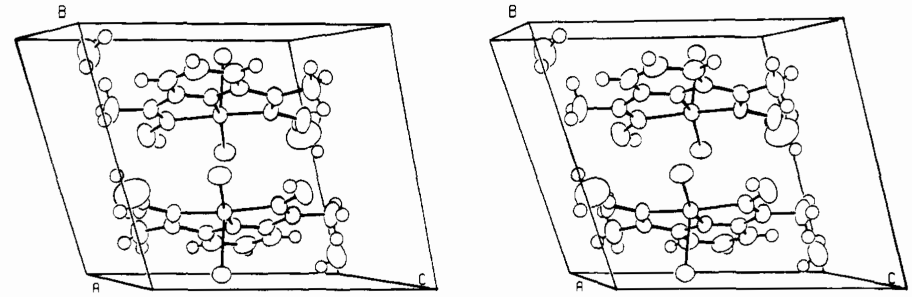

Figure 1. Stereoscopic drawing of the molecular arrangement of $Cu(DAPDH_2)Cl_2{\cdot}2H_2O$ in the triclinic $P\bar{1}$ unit cell. The thermal ellipsoids have been scaled to enclose 50% probability in this and all subsequent figures.

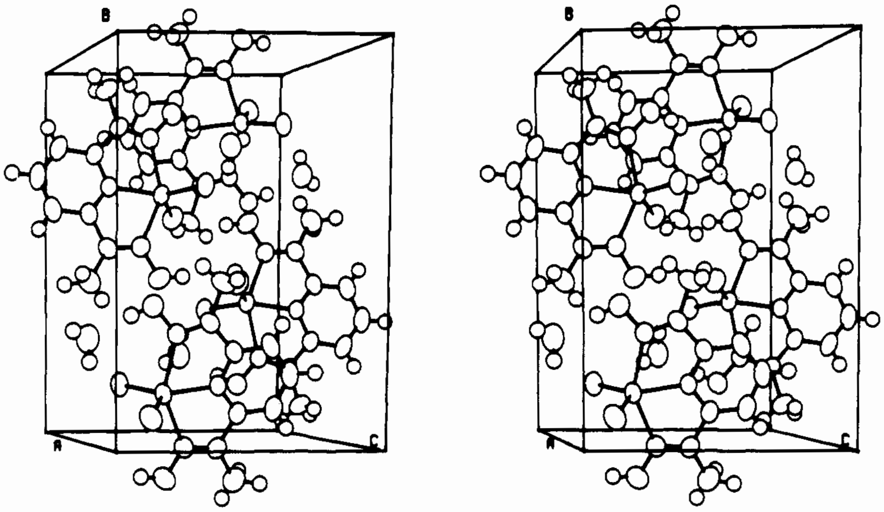

Figure 2. Stereoscopic view of the molecular arrangement of $Zn(DAPDH_2)Cl_2{\cdot}H_2O$ in the monoclinic $P2_1/n$ unit cell.

Results and Discussion

Description of the Crystal and Molecular Structures of $Cu(DAPDH_2)Cl_2{\cdot}2H_2O$ and $Zn(DAPDH_2)Cl_2{\cdot}H_2O$. The crystal structure of the dihydrate of $Cu(C_9H_{11}N_3O_2)Cl_2$ or $Cu(DAPDH_2)Cl_2$ is depicted stereographically in Figure 1, which shows the molecular arrangement of two Cu monomers and four waters of hydration in the centrosymmetric triclinic unit cell. Although at first glance the intermolecular contacts do not suggest the presence of any unusual packing effects, a closer look at the packing diagram clearly shows that each pair of copper oxime molecules is oriented in a back-to-back fashion in the unit cell. As a consequence, the Cu atom of one molecule is positioned below the sixth coordination site of the Cu atom in the other molecule. The resultant Cu···Cu separation of 4.082 (1) Å and the corresponding angles N1–Cu···Cu = 84.0 (1)°, N2–Cu···Cu = 79.9 (1)°, N3–Cu···Cu = 79.3 (1)°, Cl2–Cu···Cu = 80.4 (1)°, Cl1–Cu···Cu = 174.9 (1)° are consistent with this pairwise representation. Although the Cu···Cu separation suggests the possibility of a weak magnetic exchange between the two paramagnetic d^9 Cu(II) centers in the solid state, the bulk magnetic moment of 1.9 μ_B at room temperature[4] only deviates a small amount from that expected for an isolated $S = {}^1/_2$ system. However, since magnetic coupling involves a short-range interaction, one possibly could observe a magnetic phase transition as the Cu···Cu separation between this monomeric pair is reduced upon cooling. Another aspect of the crystal packing is the close proximity of one of the water molecules to an oxime group. The WO2(water)···H11(oxime) separation of ca. 1.94 (4) Å indicates the presence of a weak hydrogen-bonding interaction in the crystal lattice.

The crystal structure of the monohydrate of $Zn(DAPDH_2)Cl_2$ is illustrated stereographically in Figure 2. The calculated intermolecular contacts between the four Zn monomers and four waters of hydration in the monoclinic unit cell indicate that two different hydrogen-bonding interactions are probably present. One is analogous to that found in $Cu(DAPDH_2)Cl_2{\cdot}2H_2O$, with the oxygen atom of the water of hydration interacting with an oxime hydrogen atom. In this instance, the WO(water)···H11(oxime) separation of 1.78 (4) Å is noticeably shorter with WH1–WO···H11 and WH2–WO···H11 angles of 127 (4) and 117 (5)°, respectively. The second hydrogen-bonding interaction apparently involves the other oxime hydrogen atom, H1, with Cl2 of another $Zn(DAPDH_2)Cl_2$ molecule. The corresponding H1···Cl2 separation and Zn–Cl2···H1 angle are 2.15 (4) Å and 111 (1)°, respectively.

Earlier conductivity measurements[4,6] indicated that $Cu(DAPDH_2)Cl_2$ and $Zn(DAPDH_2)Cl_2$ are both nonelectrolytes, with the chlorides coordinated to produce a five-coordinate complex with $DAPDH_2$ acting as a tridentate ligand in each case. The corresponding molecular configurations for these two compounds are shown in Figure 3 with the atom-labeling schemes and appropriate bond distances and bond angles provided. For $Cu(DAPDH_2)Cl_2$, the five-coordinate environment about the central Cu(II) center resembles a distorted square pyramid. The apex of the square pyramid is occupied by a chloride ligand, and the four basal positions consist of the other chloride ligand and the three nitrogen donor atoms of the tridentate oxime ligand. A comparison of the appropriate bond distances and angles in $Cu(DAPDH_2)Cl_2$ indicates that the molecule possesses C_s symmetry with a noncrystallographic mirror plane passing through Cu, Cl1, Cl2, and N2. Although precise structural data on low-symmetry Cu(II) complexes is limited, similar structures have been proposed for 1:1 complexes of Cu with 2,2′,2″-terpyridine[21] and with 2,6-bis(2-quinolyl)pyridine[22] and have been determined for

---

[21] Harris, C. M.; Lockyer, T. N.; Stephenson, N. C. *Aust. J. Chem.* **1966**, *19*, 1741.

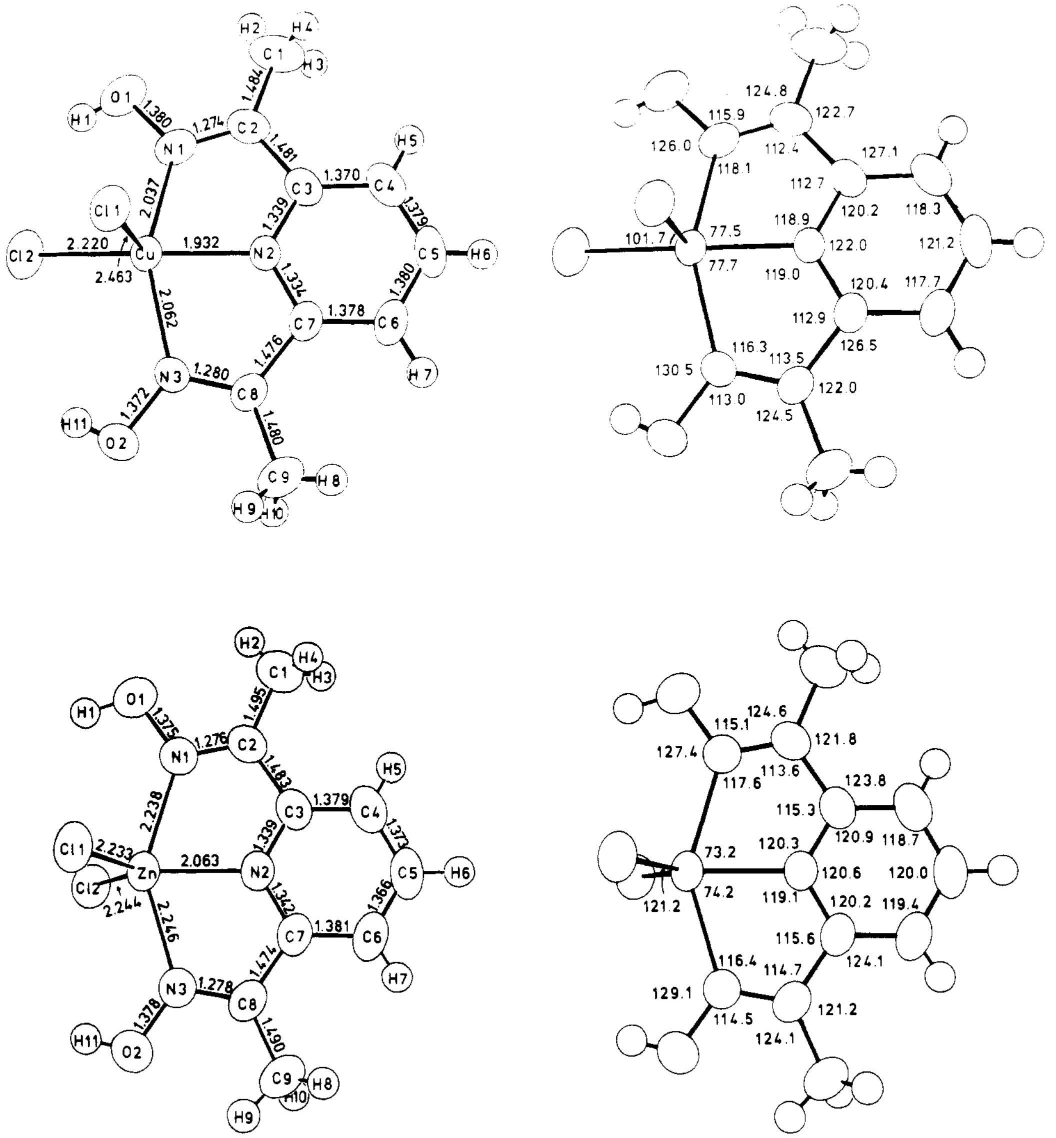

Figure 3. Molecular configurations of $Cu(DAPDH_2)Cl_2$ and $Zn(DAPDH_2)Cl_2$ with the atom-labeling schemes and pertinent bond distances and bond angles provided.

$Cu(den)(NCS)_2$ (den = $(H_2NCH_2CH_2)_2NH$)[23] and $Cu(dpt)(NCS)_2$ (dpt = $(H_2NCH_2CH_2CH_2)_2NH$).[24] A similarly distorted square-pyramidal geometry about each Cu(II) ion also exists for the binuclear $[Cu(DAPDH)]_2^{2+}$ cation.[5]

Since $(H_2NCH_2CH_2)_2NH$ and 2,6-diacetylpyridine dioxime both produce five-membered chelate rings upon metal coordination, one would expect the molecular structure of $Cu(DAPDH_2)Cl_2$ to be more comparable to that of $Cu(den)(NCS)_2$ than of $Cu(dpt)(NCS)_2$. In the former two complexes, the basal Cu–N distance opposite the monodentate Cl^- or NCS^- ligand is noticeably shorter than the remaining basal Cu–N distances. The opposite trend, however, is observed in $Cu(dpt)(NCS)_2$. The molecular packing of these complexes is also surprisingly similar, except that the Cu···Cu separations of 4.3 and 4.5 Å for $Cu(den)(NCS)_2$[23] and $Cu(dpt)(NCS)_2$[24] are somewhat longer than the observed for $Cu(DAPDH)Cl_2$. The most predominant feature of these five-coordinate copper complexes is the significantly different Cu–N(NCS) or Cu–Cl distances in each case. For example, the apical Cu–N(NCS) bond distance of 2.26 (1) Å is ca. 0.3 Å longer than the basal Cu–N(NCS) distance of 1.97 (1) Å in $Cu(den)(NCS)_2$.[23] Similarly, the apical Cu–Cl distance of 2.463 (1) Å is 0.24 Å longer than the basal Cu–Cl distance of 2.220 (1) Å in $Cu(DAPDH_2)Cl_2$. This pronounced elongation of the apical Cu–L bond in each of these five-coordinate copper complexes suggests the presence of a Jahn–Teller distortion.

Since the electronic ground state in each of these low-symmetry Cu(II) complexes is not likely to be degenerate, the observed variation in the Cu–L bond distances is probably due to second-order Jahn–Teller effects. Pearson[25] has examined this problem of molecular distortions with the aid of second-order perturbation theory and group theory. His analysis has shown for molecules with a nondegenerate ground state and low-lying excited states (within about 4 eV) that only totally symmetric motions will occur until the energy of the molecule is minimized. Thus, the bond lengths and bond angles change to produce the lowest energy configuration that still retains the original point group symmetry of the molecule. Since the molecular distortion primarily involves the lengthening of the apical Cu–L bond which lies on the molecular mirror plane,

---

(22) Wasson, J. R.; Klassen, D. M.; Richardson, H. W.; Hatfield, W. E. *Inorg. Chem.* **1977**, *16*, 1906.

(23) Cannas, M.; Carta, G.; Marongiu, G. *J. Chem. Soc., Dalton Trans.* **1974**, 553.

(24) Cannas, M.; Carta, G.; Cristini, A.; Marongiu, G. *J. Chem. Soc., Dalton Trans.* **1974**, 1278.

(25) Pearson, R. G. *J. Am. Chem. Soc.* **1969**, *91*, 4947.

Table IV. Interatomic Distances (Å) and Bond Angles (Deg) for Nonhydrogen Atoms in $Cu(C_9H_{11}N_3O_2)Cl_2{\cdot}2H_2O$ and $Zn(C_9H_{11}N_3O_2)Cl_2{\cdot}H_2O$[a]

	M = Cu	M = Zn
	A. Interatomic Distances	
M-Cl1	2.463 (1)	2.233 (1)
M-Cl2	2.220 (1)	2.244 (1)
M-N1	2.037 (3)	2.238 (2)
M-N2	1.932 (3)	2.063 (2)
M-N3	2.062 (3)	2.246 (2)
N1-O1	1.380 (5)	1.375 (4)
N3-O2	1.372 (4)	1.378 (3)
N1-C2	1.274 (5)	1.276 (4)
N3-C8	1.280 (5)	1.278 (4)
C1-C2	1.484 (7)	1.495 (6)
C8-C9	1.480 (7)	1.490 (5)
C2-C3	1.481 (5)	1.483 (4)
C7-C8	1.476 (5)	1.474 (4)
N2-C3	1.339 (4)	1.339 (4)
N2-C7	1.334 (5)	1.342 (4)
C3-C4	1.370 (5)	1.379 (4)
C6-C7	1.378 (5)	1.381 (4)
C4-C5	1.379 (6)	1.373 (6)
C6-C5	1.380 (6)	1.366 (5)
	B. Bond Angles	
Cl1-M-Cl2	101.73 (3)	121.17 (3)
Cl1-M-N1	100.5 (1)	95.90 (6)
Cl1-M-N2	98.4 (1)	122.11 (7)
Cl1-M-N3	95.6 (1)	100.37 (7)
Cl2-M-N1	93.9 (1)	96.66 (7)
Cl2-M-N2	159.2 (1)	116.56 (7)
Cl2-M-N3	105.1 (1)	98.76 (6)
N1-M-N2	77.5 (1)	73.18 (9)
N2-M-N3	77.7 (1)	74.15 (8)
M-N1-O1	126.0 (2)	127.4 (2)
M-N3-O2	130.5 (2)	129.1 (2)
M-N1-C2	118.1 (3)	117.6 (2)
M-N3-C8	116.3 (2)	116.4 (2)
O1-N1-C2	115.9 (3)	115.1 (2)
O2-N3-C8	113.0 (3)	114.5 (2)
N1-C2-C1	124.8 (5)	124.6 (3)
N3-C8-C9	124.5 (4)	124.1 (3)
C1-C2-C3	122.7 (4)	121.8 (3)
C7-C8-C9	122.0 (4)	121.2 (3)
C2-C3-N2	112.7 (3)	115.3 (2)
C8-C7-N2	122.9 (3)	115.6 (2)
C2-C3-C4	127.1 (3)	123.8 (3)
C6-C7-C8	126.5 (3)	124.1 (3)
M-N2-C3	118.9 (2)	120.3 (2)
M-N2-C7	119.0 (2)	119.1 (2)
N2-C3-C4	120.2 (3)	120.9 (3)
N2-C7-C6	120.4 (3)	120.2 (3)
C3-C4-C5	118.3 (4)	118.7 (3)
C5-C6-C7	117.7 (4)	119.4 (4)
C3-N2-C7	122.0 (3)	120.6 (2)
C4-C5-C6	121.2 (4)	120.0 (3)

[a] The esd's given in parentheses for the interatomic separations and bond angles were calculated from the standard errors in the fractional coordinates of the corresponding atomic positions.

this distortion does not alter the C_s symmetry of these molecules.

For $Zn(DAPDH_2)Cl_2$ the five-coordinate environment about the central Zn(II) ion can be viewed as a distorted trigonal bipyramid, with the equatorial positions occupied by Cl1, Cl2, and N2 and the apical positions occupied by the oxime N atoms, N1 and N3. The bond angles within this equatorial plane are nearly 120°, and the oxime N atoms are symmetrically disposed above and below the plane. This ligand disposition in $Zn(DAPDH_2)Cl_2$ is consistent with C_{2v} point group symmetry for the molecule. In contrast to $Cu(DAPDH_2)Cl_2$, which is unstable to elongation of the apical M–Cl bond, $Zn(DAPDH_2)Cl_2$ is not. The Zn–Cl bond distances of 2.233 (1) and 2.244 (1) Å are equivalent for all practical purposes, as expected for a d^{10} complex.

Table V. M–N Bond Distances (Å) and N–M–N Bond Angles (Deg) in Metal Complexes of 2,6-Diacetylpyridine Dioxime

ref	compd	M–N(oxime)	M–N(py)	N(oxime)–M–N(py)
29	$Ni(DAPD)_2$	1.973 (3)	1.837 (4)	82.4 (1)
5	$[Cu(DAPDH)]_2(BF_4)_2{\cdot}2H_2O$	2.023 (4)	1.924 (4)	76.9 (2)
		2.081 (4)		79.3 (2)
		2.029 (4)	1.905 (4)	77.8 (2)
		2.064 (4)		79.8 (2)
this work	$Cu(DAPDH_2)Cl_2{\cdot}2H_2O$	2.037 (3)	1.932 (3)	77.5 (1)
		2.062 (3)		77.7 (1)
this work	$Zn(DAPDH_2)Cl_2{\cdot}H_2O$	2.238 (2)	2.063 (2)	73.2 (1)
		2.246 (2)		74.2 (1)

To the best of our knowledge, the only other structural analysis of a similar five-coordinate Zn complex with one tridentate ligand and two monodentate ligands that has been reported in the literature is that described by Einstein and Penfold[26] for $Zn(terpy)Cl_2$, where terpy = 2,2′,2″-terpyridine. Their refinement was performed with use of film data furnished by Corbridge and Cox.[27] Despite the limited accuracy of the X-ray diffraction data, their analysis unequivocally established the gross features of the molecular structure. Although the coordination environments about the Zn(II) ion in $Zn(DAPDH_2)Cl_2$ and $Zn(terpy)Cl_2$ are comparable, the orientations of the tridentate ligand with respect to the $ZnCl_2$ moiety substantially differ. For example, the Cl–Zn–N2 bond angles are 122.11 (7) and 116.56 (7)° in $Zn(DAPDH_2)Cl_2$ compared to 105 and 145° in $Zn(terpy)Cl_2$. This wider difference in the latter complex reflects a systematic departure from planarity for the coordinated terpyridyl group.[28]

Nature of the Metal–Oxime Interaction. Our structural studies of $Cu(DAPDH_2)Cl_2$, $Zn(DAPDH_2)Cl_2$, and the binuclear $[Cu(DAPDH)]_2^{2+}$ species have provided an opportunity to examine two different modes of oxime coordination available to 2,6-diacetylpyridine dioxime. Whereas this oxime ligand behaves as an unsymmetrical tetradentate chelate in $[Cu(DAPDH_2)]_2^{2+}$, it coordinates as a symmetrical tridentate chelate in $Cu(DAPDH_2)Cl_2$ and $Zn(DAPDH_2)Cl_2$. An examination of the metal–nitrogen bond distances in Table V indicates that, in all metal complexes of 2,6-diacetylpyridine dioxime for which structural data is available, the two M–N(oxime) bonds are ca. 0.1–0.2 Å longer than the corresponding M–N(py) bond within each metal–tridentate chelate unit. This structural feature contrasts with that observed by Schlemper and co-workers for tetradentate α-amine oxime[30,31] and trinuclear Cu(II) oxime complexes.[32] In these particular systems the trend is reversed with the Cu–N(oxime) distances consistently 0.03–0.07 Å shorter than the interior Cu–N(amine) distances. The larger variation in the M–N(oxime) bond distances observed for $[Cu(DAPDH)]_2^{2+}$ is probably a consequence of the dioxime's unsymmetrical mode of coordination.

On the basis of the estimated "effective" ionic radii for Cu^{2+} (0.65 Å) and Zn^{2+} (0.68 Å) in a five-coordinate environment,[33] the corresponding M–N and M–Cl bond distances in $Cu(DAPDH_2)Cl_2$ and $Zn(DAPDH_2)Cl_2$ would be expected to be fairly similar in magnitude. In terms of the M–Cl distances, this premise is clearly supported by a comparison of the basal

---

(26) Einstein, F. W. B.; Penfold, B. R. *Acta Crystallogr.* **1966**, *20*, 924.
(27) Corbridge, D. E. C.; Cox, E. G. *J. Chem. Soc.* **1956**, *159*, 594.
(28) Goldschmied, E.; Stephenson, N. C. *Acta Crystallogr., Sect. B* **1970**, *B26*, 1867.
(29) Sproul, G.; Stucky, G. *Inorg. Chem.* **1973**, *12*, 2899.
(30) Liss, I. B.; Schlemper, E. O. *Inorg. Chem.* **1975**, *14*, 3035.
(31) Gavel, D. P.; Schlemper, E. O. *Inorg. Chem.* **1979**, *18*, 283.
(32) Ross, P. F.; Murmann, R. K.; Schlemper, E. O. *Acta Crystallogr., Sect. B* **1974**, *B30*, 1120.
(33) Shannon, R. D.; Prewitt, C. T. *Acta Crystallogr., Sect. B* **1969**, *B25*, 925.

Cu–Cl distance in $Cu(DAPDH_2)Cl_2$ and the Zn–Cl distances in $Zn(DAPDH_2)Cl_2$, which differ by ca. 0.02 Å. For the M–N distances a substantially different situation exists. The Zn–N(py) and Zn–N(oxime) bond distances in $Zn(DAPDH_2)Cl_2$ are ca. 0.13 and 0.20 Å longer than their respective Cu–N bond distances in $Cu(DAPDH_2)Cl_2$. These unusually long Zn–N bond distances strongly suggest that the angular overlap between the available metal orbitals and the oxime's N donor orbitals is relatively poor in this five-coordinate Zn complex. This remark indicates that it may be possible to enhance the Zn–N bonding interaction by using a tridentate ligand such as $(H_2NCH_2CH_2)_2NH$, which possesses a more flexible chelate backbone than $DAPDH_2$.

The molecular configuration associated with these five-coordinate complexes appears to have a noticeable influence upon the planarity of the coordinated dioxime ligand as well. In both $Cu(DAPDH_2)Cl_2$ and $[Cu(DAPDH)]_2^{2+}$ the dioxime ligand is not strictly planar. All of the nonhydrogen atoms of the tridentate ligand are displaced below the plane defined by the three N donor atoms and away from the copper atom which lies 0.289 (1) and ca. 0.19 (1) Å above this plane in $Cu(DAPDH_2)Cl_2$ and $[Cu(DAPDH)]_2^{2+}$, respectively. In contrast, for $Zn(DAPDH_2)Cl_2$ the corresponding deviations from planarity are significantly smaller and the Zn atom lies in the plane of the oxime ligand.

The bond distances and bond angles within the coordinated oxime ligands in $Cu(DAPDH_2)Cl_2$, $Zn(DAPDH_2)Cl_2$, and $[Cu(DAPDH)]_2^{2+}$ species are comparable in magnitude despite the observed differences in the mode of oxime coordination. The orbital hybridizations about the N donor atoms and the carbon atoms of the relatively rigid backbone of this chelate ligand are essentially sp^2. The average N–OH distance of 1.376 Å in $Cu(DAPDH_2)Cl_2$ and $Zn(DAPDH_2)Cl_2$ are comparable to that of 1.39 Å in $[Cu(DAPDH)]_2^{2+}$.[5] Deprotonation of the oxime, however, is accompanied by a significant reduction in the N–O bond distance. The average N–O bond distance is reduced from ca. 1.38 Å for $DAPDH_2$ in $M(DAPDH_2)Cl_2$ to ca. 1.33 Å for $DAPDH^-$ in $[Cu(DAPDH)]_2^{2+}$. For the doubly deprotonated $DAPD^{2-}$ chelates of $Ni(DAPD)_2$,[29] a substantially shorter N–O distance of 1.257 (3) Å was determined.

Finally, the N(oxime)–M–N(py) bond angle for the five-membered rings of these dioxime complexes (Table V) is closely related to the magnitude of the M–N(py) bond. As the M–N(py) distance increases from 1.837 (4) Å for $Ni(DAPD)_2$[29] to 1.932 (3) Å for $Cu(DAPDH_2)Cl_2$ to 2.063 (2) Å for $Zn(DAPDH_2)Cl_2$, the corresponding inner "bite" angle decreases continually from 82.4 (1) to 77.6 (average) to 73.7° (average), respectively. In $Ni(DAPD)_2$ the higher oxidation state and smaller size of the Ni(IV) ion cause the chelating oxime groups to be pulled more strongly toward the nickel. This distortion of the $DAPD^{2-}$ ligand is accompanied by a noticeable increase in the N(oxime)–M–N(py) bond angle. Conversely, the weaker metal–oxime interaction in $Zn(DAPDH_2)Cl_2$ is characterized by substantially longer M–N bond distances which distort the coordinated $DAPDH_2$ ligand in the opposite sense as reflected by a reduction of the average N(oxime)–M–N(py) bond angle.

Acknowledgment. Computer time for the refinement of the X-ray diffraction data was provided by the West Virginia Network for Educational Telecomputing.

Registry No. $Cu(DAPDH_2)Cl_2 \cdot 2H_2O$, 82310-79-0; $Zn(DAPDH_2)Cl_2 \cdot H_2O$, 82265-78-9.

Supplementary Material Available: Tables of refined thermal parameters, hydrogen-bond distances, specific least-squares planes, and observed and calculated structure factors (22 pages). Ordering information is given on any current masthead page.

Contribution from the Departments of Chemistry, Oregon State University, Corvallis, Oregon 97331,
and University of Reading, Whiteknights, Reading, Berkshire, England

Gas-Phase Electron-Diffraction Studies of the Molecular Structures of Tetrachlorosulfidotungsten(VI), $WSCl_4$, and Tetrachloroselenotungsten(VI), $WSeCl_4$

ELIZABETH M. PAGE,[1a] DAVID A. RICE,[1a] KOLBJØRN HAGEN,[1b,c] LISE HEDBERG,[1c]
and KENNETH HEDBERG*[1c]

Received December 28, 1981

The molecular structures of $WSCl_4$ and $WSeCl_4$ have been studied by gas-phase electron diffraction at average nozzle temperatures of 200 and 220 °C, respectively. The experimental data for both species are fitted by square-pyramidal models of C_{4v} symmetry in which the tungsten atom is slightly above the plane of the four chlorine atoms. The following principal distances (r_a), angles, and root-mean-square amplitudes of vibration (l) with estimated uncertainties of 2σ were obtained. $WSCl_4$: $r(W{=}S) = 2.086\ (6)$ Å, $r(W{-}Cl) = 2.277\ (3)$ Å, $\angle SWCl = 104.2\ (5)°$, $\angle ClWCl = 86.5\ (2)°$, $l(W{=}S) = 0.031\ (6)$ Å, $l(W{-}Cl) = 0.058\ (4)$ Å, $l(S{\cdot}Cl) = 0.147\ (17)$ Å, $l(Cl{\cdot}Cl) = 0.114\ (10)$ Å, $l(Cl{\cdot\cdot}Cl) = 0.120\ (25)$ Å. $WSeCl_4$: $r(W{=}Se) = 2.203\ (4)$ Å, $r(W{-}Cl) = 2.284\ (3)$ Å, $\angle SeWCl = 104.4\ (3)°$, $\angle ClWCl = 86.5\ (2)°$, $l(W{=}Se) = 0.055\ (4)$ Å, $l(W{-}Cl) = 0.060\ (3)$Å, $l(Se{\cdot}Cl) = 0.147\ (9)$ Å, $l(Cl{\cdot}Cl) = 0.116\ (8)$ Å, $l(Cl{\cdot\cdot}Cl) = 0.116\ (19)$ Å. The similarities and differences of these structures, together with that of $WOCl_4$ available in the literature, are interpreted in terms of relative bond orders and nonbond repulsions.

Introduction

The molecular structures in the gas phase of a number of oxo halides of group 6B elements are known from electron-diffraction measurements. Nothing is known about the structures of the analogous sulfido and seleno halides, but it is reasonable to expect the molecules to have C_{4v} symmetry as do the oxygen compounds. Should this be the case, the structural differences resulting from substitution at the axial position in these compounds permit insights into the nature of the bonding operating in them. Accordingly we decided to investigate the structures of $WSCl_4$ and $WSeCl_4$ by electron diffraction. Structural data are already available for $WOCl_4$.[2]

There are apparently no measurements of the vibrational spectra of $WSCl_4$ or $WSeCl_4$ in the literature, but such data do exist for $WOCl_4$.[3,4] Other information includes X-ray

---

[1] (a) University of Reading. (b) On leave from the University of Trondheim, Trondheim, Norway. (c) Oregon State University.

[2] (a) Iijima, K.; Shibata, S. *Bull. Chem. Soc. Jpn.* **1974**, *47*, 1393. (b) Zharskii, I. M.; Novikov, G. I.; Zasorin, E. Z.; Spiridonov, V. P. *Dokl. Akad. Nauk BSSR* **1976**, *20*, 234.

[3] Ward, B. G.; Stafford, F. E. *Inorg. Chem.* **1968**, *7*, 2569.